Reprinted from

thin solid films

Thin Solid Films 330 (1998) 7–13

Effective interaction and density profiles of confined charged colloids

Anne M. Denton[a], Hartmut Löwen[a,b,*]

[a]*Institut fur Theoretische Physik II, Heinrich-Heine-Universität Dusseldorf, Universitätsstraße 1, D-40225 Dusseldorf, Germany*
[b]*Institut fur FestLorperforschung, Forschungszentrum Julich, D-52425 Julich, Germany*

ELSEVIER

THIN SOLID FILMS

Types of Contributions
– original papers not previously published
– invited review articles
– letters, 1800–2500 words
– announcements, reports on conferences, news

A pamphlet containing more detailed instructions on the preparation of manuscripts for THIN SOLID FILMS may be obtained from the publisher in Oxford.

Sections
The journal is divided into the following sections.

A. **Synthesis and Characterization**: nucleation and growth from the gas, liquid and solid phases; microstructural and microchemical film characterization; new concepts and techniques for film synthesis, modification, processing and characterization.

B. **Surfaces, Interfaces and Colloidal Behaviour**: surface and interface phenomena: physics, chemistry and applications.

C. **Metallurgical, Protective and Hard Layers**: fundamental aspects of layers and coatings used in diffusion barrier, corrosion, high-temperature, wear, erosion, and other extreme environments.

D. **Mechanics and Nanomechanics of Thin Layers**: mechanical properties of thin layers and nanoscale structures; surface forces; micro- and nanoengineering.

E. **Electronics, Optics and Opto-electronics**: synthesis, properties and processing of layers used in electronic, optical and opto-electronic applications; device engineering.

F. **Magnetics and Magneto-optics**: fundamental aspects of layers used in magnetic and magneto-optic applications; magnetic, optical and magneto-optical recording devices.

G. **Superconductivity**: synthesis and properties of layers used in superconducting applications.

H. **Langmuir–Blodgett, Biological and Related Films**: synthesis and properties of Langmuir–Blodgett, biological and related layers: device applications.

I. **Thin Film Devices, Sensors and Actuators**: fabrication, processing and properties of devices including sensors and actuators based upon thin layers.

J. **Condensed Matter Film Behaviour**: interdisciplinary and multidisciplinary topics.

Submission of Papers
Manuscripts (original, two clear copies and accompanying diskette (MS-DOS or MAC format)) should be sent to:
EDITORIAL OFFICE (UK) OF *THIN SOLID FILMS*
Elsevier Science Ltd
The Boulevard, Langford Lane
Kidlington
Oxford, OX5 1GB, UK

To ensure an optimal refereeing process, we ask authors to provide, together with the manuscript, a list of 3 to 5 potential reviewers and their addresses/e-mail.

All the authors of a paper should sign the covering letter. Contributions are accepted on the understanding that the authors have obtained the necessary authority for publication. Submission of a manuscript implies that it is not under consideration for publication elsewhere.

Frequency
20 volumes in 1998, two issues per volume.

Subscription Information 1998
Volumes 312–331, each volume containing 2 issues, are scheduled for publication. Prices are available from the publisher upon request. Subscriptions are accepted on a prepaid basis only. Issues are sent by SAL (Surface Air Lifted) mail wherever this service is available. Airmail rates are available upon request.

Orders, claims, and product enquiries: please contact the Customer Support Department at the Regional Sales Office nearest you:

New York
Elsevier Science
P.O. Box 945
New York, NY 10159-0945, USA
Tel.: (+1) 212-633-3730
[Toll free number for North American customers: 1-888-4ES-INFO (437-4636)]
Fax: (+1) 212-633-3680
E-mail: usinfo-f@elsevier.com

Amsterdam
Elsevier Science
P.O. Box 211
1000 AE Amsterdam
The Netherlands
Tel.: (+31) 20-4853757
Fax: (+31) 20-4853432
E-mail: nlinfo-f@elsevier.nl

Tokyo
Elsevier Science K.K.
9-15 Higashi-Azabu 1-chome
Minato-ku, Tokyo 106-0044
Japan
Tel.: (+81) 3-5561-5033
Fax: (+81) 3-5561-5047
E-mail: info@elsevier.co.jp

Singapore
Elsevier Science
No. 1 Temasek Avenue
#17-01 Millenia Tower
Singapore 039192
Tel.: (+65) 434-3727
Fax: (+65) 337-2230
E-mail: asiainfo@elsevier.com.sg

Rio de Janeiro
Elsevier Science
Rua Sete de Setembro 111/16 Andar
20050-002 Centro
Rio de Janeiro - RJ
Brazil
Tel.: (+55) 21-509-5340
Fax: (+55) 21-507-1991
E-mail: elsevier@campus.com.br
[Note (Latin America): for orders, claims and help desk information, please contact the Regional Sales Office in New York as listed above]

ELSEVIER

Thin Solid Films 330 (1998) 7–13

thin solid films

Effective interaction and density profiles of confined charged colloids

Anne M. Denton[a], Hartmut Löwen[a,b,*]

[a]*Institut fur Theoretische Physik II, Heinrich-Heine-Universität Dusseldorf, Universitätsstraße 1, D-40225 Dusseldorf, Germany*
[b]*Institut fur FestLorperforschung, Forschungszentrum Julich, D-52425 Julich, Germany*

Abstract

The interaction between charged colloidal particles confined between two parallel charged plates is investigated theoretically. We propose a simple model with a space-dependent Yukawa pair potential between the colloids which is derived from lineal screening and density functional perturbation theory. Within this model, the density profile of the confined colloidal particles is obtained by computer simulation. In the absence of van der Waals attractions between the walls and the colloidal particles, there is no practical difference in the colloidal density profiles as compared with those obtained with the usual space-independent Yukawa pair potential. However, there can be large deviations if an additional large wall attraction is present. © 1998 Elsevier Science S.A. All rights reserved

Keywords: Charged colloid; Molecular dynamics; Confinement; Density functional theory

1. Introduction

Charged colloids confined between two parallel glass plates have the intriguing property that their positions can be watched in real space by video microscopy (see e.g. Refs. [1,2]). This allows for a direct determination of their pair structure and their Brownian trajectories. For highly charged plates and highly charged colloidal particles, there is effectively only one colloidal layer providing an excellent realisation of a strictly two-dimensional system [3]. It is known that the freezing transition in two spatial dimensions can be mediated by a hexatic phase [4]. Hence, colloidal monolayers represent important samples for a search for such a hexatic phase with long-ranged bond orientational order [5–12].

The aim of this paper is to investigate and discuss the effective interaction between the charged colloids if they are strongly confined between highly charged plates. The effective interaction has gained considerable interest recently since experiments reveal the possibility of an attraction between colloidal particles close to the wall [13–17]. The interpretation of the experiments is, however, still not unambiguous and there is not any clear hint from theory that an effective attraction takes place.

Almost every theoretical approach for the effective interactions adopts linear screening theory for colloids heavily confined to the mid-plane in between the plates. The dominant term then is a two-dimensional Yukawa pair potential $\propto \exp(-\kappa r)/r$ [18–21] where r is the lateral interparticle separation and the inverse Debye–Hückel screening constant κ is dominated by the counterion concentration in the mid-plane. This 2-dimensional Yukawa model was extensively used in subsequent computer simulations for the structural correlations [22–26], the Brownian dynamics [22,23,27–29], and the freezing transitions in two-dimensional fluids [30]. In this paper, we generalise this result taking into account the non-uniformity of the counterionic density profile in the direction z perpendicular to the plates.

Consequently we obtain a space-dependent Yukawa pair potential which depends not only on the difference between the two particle positions but also on the positions themselves In fact, the inverse screening constant κ now depends explicitly on the z-coordinates, Z_1 and Z_2, of the colloidal pair. We adopt linear screening theory as formulated recently in the density functional language [31] and use density functional perturbation theory to obtain an explicit expression for this space-dependent pair potential. We then explore the density profile of the colloidal particle by computer simulation.

It turns out that the density profile is reduced in the mid-plane if the z-dependent κ is used as compared to the traditional case of constant κ. Intuitively this is expected since

* Corresponding author. Fax: +49 211 8112262; e-mail: hlowen@thphy.uni-duesseldorf.de

0040-6090/98/$ - see front matter
PII S0040-6090(98)00794-9

the screening becomes more effective close to the plates due to the increased amount of counterions from the charged wall and hence the particles explore closer wall distances. The deviation from the Yukawa potential can become particularly pronounced if an additional van der Waals attraction between the walls and the colloidal particles is present.

The paper is organised as follows. In Section 2, we define our model deriving the space-dependent Yukawa pair potential from density functional theory. Then we present our results in Section 3. We conclude in Section 4.

2. Derivation of the model

In order to derive the effective interaction between confined charged colloids, we proceed in four steps. We first consider a situation without any macroions, i.e. the number of macroions N_m is zero. Then we subsequently discuss a single macroion ($N_m = 1$), a pair of macroions ($N_m = 2$), and finally an arbitrary number N_m of macroions. In all of our considerations, there is no added salt, and the macroion radius is set to zero, i.e. the spatial extension of the macroions is much smaller than the local Debye–Hückel screening length. The general situation is sketched in Fig. 1: Two parallel plates each of them carrying a homogeneous surface charge density σ are a distance $2L$ apart. The surface charge comes from dissociated counterions with a charge qe where q is the valency and e the elementary charge. In between, there is a microscopic solvent with a dielectric constant ϵ and N_m macroions each of them carrying a charge Ze and provide a total number of $N_m|Z/q|$ additional oppositely charged counterions which are indistinguishable from those coming from the charged plates. The spatial coordinate perpendicular to the plates is denoted with z. The origin $z = 0$ coincides with the position of the left plate. The macroion positions are given by $\{\vec{r}_i\}$, where $i = 1,..., N_m$ labels the macroions. Their z-coordinates are denoted with Z_i.

2.1. Density profile of counterions without any macroion

This case is well-studied since the early theoretical foundations of colloid science; see e.g. the textbooks ([32]; for a review see [33]). The Poisson–Boltzmann (PB) theory for the counterions can be solved analytically for a situation of two equally charged plates. In the salt-free case, the mean number density of counterions stemming from the charged walls is fixed by global charge neutrality to

$$\bar{\rho}_0 = \frac{\sigma}{qeL} \tag{1}$$

The inverse Debye–Hückel screening length κ_0 is then defined via

$$\kappa_2^0 = \frac{4\pi(qe)2\bar{\rho}_0}{\epsilon k_B T} \tag{2}$$

where k_BT is the thermal energy. Within PB theory, the z-dependent inhomogeneous number density profile $\rho_w(z)$ of the counterions is given by

$$\rho_w(z) = \bar{\sigma}_0 \frac{2\gamma_0^2}{(\kappa_0 L)^2} \frac{1}{\cos^2(\gamma_0(1 - z/L))} \tag{3}$$

where the index w indicates that the counterions are solely coming from the charged walls. The constant In is implicitly given as the solution of the transcendental equation

$$\frac{(\kappa_0 L)^2}{2\gamma_0^2} - \tan\gamma_0 = 0 \quad \gamma_0 \in \left[0, \frac{\pi}{2}\right] \tag{4}$$

A typical counterion density profile $\rho_w(z)$ is shown in Fig. 2. Note that for very hip surface charge densities σ the midplane counterion density saturates at a constant value since most of the counterions condense in a Stern-layer close to the plates. Explicitly, $\rho_w(z \equiv L) \to \pi/8L^2\lambda_B$ as $|\sigma| \to \infty$ with $\lambda_B = (qe)^2/k_BT\epsilon$ being the Bjerrum length of the counterions.

The corresponding electric potential $\phi(z)$ reads

$$\phi(z) = -\frac{2k_BT}{|qe|}\ln(\cos(\gamma_0(1 - z/L))) \tag{5}$$

This potential is normalised such that it vanishes for the midplane ($z \equiv L$) between the plates. For $z \approx L$, it can be approximated by a parabola

$$\phi(z) = -\frac{2k_BT}{|qe|}\gamma_0^2\left(\frac{z-L}{L}\right)^2 + O(((z-L)/L)^4) \tag{6}$$

A typical shape of $\phi(z)$ together with its parabolic approximation is shown in Fig. 3.

We note that these results can be derived alternatively from density functional theory [31]. In fact, $\rho_w(z)$ *is* the density profile that minimises the Helmholtz free energy functional $\mathcal{F}_0[\rho(\vec{r})]$ with respect to $\rho(\vec{r})$ under the constraint of fixed average density

$$\int_A \int_0^{2L} d^3r\rho(\vec{r}) \equiv \int_\Omega d^3r\rho(\vec{r}) = \bar{\rho}_0\Omega \tag{7}$$

Here, $\Omega = 2LA$ is the total system volume and A is the area of one plate. $\mathcal{F}_0[\rho(\vec{r})]$ consists of three terms

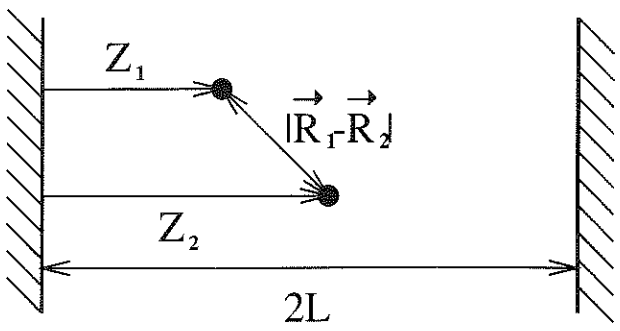

Fig. 1. Schematic diagram of a colloidal suspension between parallel walls. The distance between particles 1 and 2 is denoted by $|\vec{R}_1 - \vec{R}_2|$, their distance from one wall by Z_1 and Z_2, and the separation of the walls by $2L$.

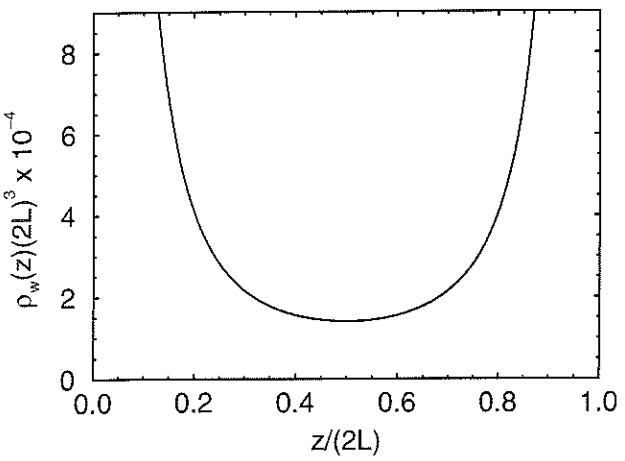

Fig. 2. Density distribution $\rho_w(z)$ of counterions between walls of surface charge density $\rho = 12.8e/\text{nm}^2$, separated by a distance $2L = 0.005$ cm. It was determined from Poisson Boltzmann theory and used as a reference density in the simulations.

$$\mathcal{F}_0[\rho(\vec{r})] = \mathcal{F}^{(1)}[\rho(\vec{r})] + \mathcal{F}^{(2)}[\rho(\vec{r})] + \mathcal{F}^{(3)}[\rho(\vec{r})] \tag{8}$$

The first term $\mathcal{F}^{(1)}[\rho(\vec{r})]$ is the entropy from an ideal counterion gas which is a local but nonlinear functional

$$\mathcal{F}^{(1)}[\rho(\vec{r})] = k_B T \int_\Omega d^3 r \rho(\vec{r})[\ln(\Lambda^3 \rho(\vec{r})) - 1] \tag{9}$$

Λ denoting the thermal de Broglie wavelength of the counterions. The second term, $\mathcal{F}^{(2)}[\rho(\vec{r})]$, describes the linear external coupling to the plates,

$$\mathcal{F}^{(2)}[\rho(\vec{r})] = \int_\Omega d^3 r \rho(\vec{r}) V_w(z) \tag{10}$$

which ensures vanishing counterion density profiles beyond the plates since

$$V_w(z) = \begin{cases} \infty \text{ for } z < 0 \text{ and } z > 2L \\ 0 \text{ for } 0 \le z \le 2L \end{cases} \tag{11}$$

When the integration is confined to the physically accessible volume Ω, then: $\mathcal{F}^{(2)}$ vanishes. We nevertheless formally keep this term since different wall–counterion interactions could be described more flexibly then. Finally the Coulomb coupling between the counterions is taken into account via the nonlocal mean-field term which is quadratic in $\rho(\vec{r})$:

$$\mathcal{F}^{(3)}[\rho(\vec{r})] = \frac{1}{2}\int_\Omega d^3 r \int_\Omega d^3 r' \rho(\vec{r}) \rho(\vec{r}\,') \frac{(qe)2}{\epsilon |\vec{r} - \vec{r}\,'|} \tag{12}$$

In the following we shall use the more flexible density functional language to extract the effective interactions.

2.2. A single macroion between charged plates

Let us now consider a single macroion with a position $\vec{r}_1 = (X_1, Y_1, Z_1)$ $(0 \le Z_1 \le 2L)$. The total free energy density functional $\mathcal{F}([\rho(\vec{r})], \{\vec{r}\})$ which has to be minimised, with respect to the counterion density profile now involves $\mathcal{F}_0([\rho(\vec{r})]$ and the additional Coulomb coupling of the counterions to the macroion which we denote by $\mathcal{F}^{(4)}([\rho(\vec{r})], \{\vec{R}_1\})$. Hence,

$$\mathcal{F}([\rho(\vec{r})]) = \mathcal{F}_0[\rho(\vec{r})] + \mathcal{F}^{(4)}([\rho(\vec{r})], \{\vec{R}_1\}) \tag{13}$$

with

$$\mathcal{F}^{(4)}([\rho(\vec{r})], \{\vec{r}_1\}) = \int_\Omega d^3 r \rho(\vec{r}) V_{mc}(|\vec{r} - \vec{r}_1|) \tag{14}$$

where

$$V_{mc}(r) = \frac{-|Zq|e^2}{\epsilon r} \tag{15}$$

is the macroion–counterion interaction. An analytic minimisation of $\mathcal{F}([\rho(\vec{r})], \{\vec{R}_1\})$ is not possible, since the problem is not any longer translational invariant in lateral direction. We assume, however, that the actual minimum is close to the former (macroion-free) PB solution given by Eq. (3). In particular, this is justified if most of the counterions in the solution are stemming from the charged plates. Hence we take $\rho_w(z)$ as a reference density and expand the nonlinear functional $\mathcal{F}^{(1)}[\rho(\vec{r})]$ quadratically around this reference density [31]:

$$\mathcal{F}^{(1)}[\rho(\vec{r})] \approx k_B T \int_\Omega d^3 r \{\rho_w(z) \ln(\Lambda^3 \rho_w(z)) +$$

$$\ln(\Lambda^3 \rho_w(z))(\rho(\vec{r}) - \rho_w(z)) + \frac{1}{2\rho_w(z)}(\rho(\vec{r}) - \rho_w(z))^2\} \tag{16}$$

Within this quadratic approximation, the minimising condition for $\mathcal{F}([\rho(\vec{r})], \{\vec{R}_1\})$ becomes linear

$$k_B T \frac{\Delta(\vec{r})}{\rho_w(z)} + V_{mc}(|\vec{r} - \vec{R}_1|) + \int_\Omega d^3 r' \Delta(\vec{r}') \frac{(qe)2}{\epsilon |\vec{r} - \vec{r}'|} + \mu = 0 \tag{17}$$

where the density difference $\Delta(\vec{r}) \equiv \rho(\vec{r}) - \rho_w(z)$ is the unknown function and μ is a Lagrange multiplier ensuring global charge neutrality. Due to the term $k_B T(\Delta(\vec{r})/\rho_w(z))$ this integral equation cannot be solved analytically. We hence adopt a further 'adiabatic' approximation assuming that $\rho_w(Z)$ is slowly varying in the region where the additional counterions from the macroions are located around the macroion, i.e. in the region where $\Delta(\vec{r})$ is nonvanishing. This allows us to set $k_B T(\Delta(\vec{r})/\rho_w(z)) \approx k_B T(\Delta(\vec{r})/\rho_w(Z_1))$ in Eq. (17). Now, by Fourier transformation, we obtain $\Delta(\vec{r})$ as

$$\Delta(\vec{r}) \equiv \Delta^{(0)}(\vec{r}, \vec{R}_1) = \frac{Z}{q} \frac{\kappa(Z_1)}{4\pi} \frac{\exp(-\kappa^2(Z_1)|\vec{r} - \vec{R}_1|)}{|\vec{r} - \vec{R}_1|} \tag{18}$$

where the Z_1-dependent inverse Debye–Hückel screening length is now given by

$$\kappa(Z_1)^2 = \frac{4\pi(qe)^2 \rho w(Z_1)}{\epsilon k_B T} \tag{19}$$

This shows a posteriori that our adiabatic approximation is reasonable as long as the particle is not too close to the plates such that its Yukawa orbital does not penetrate into the walls. Clearly, the extension of the Yukawa-density-

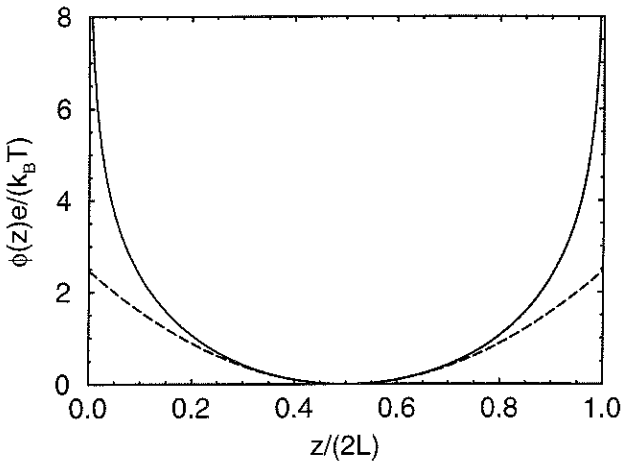

Fig. 3. Electrostatic potential $\phi(z)$ due to the wall counterion distribution in Fig. 2 (solid curve) and the parabolic approximation to it (dashed curve).

orbital (Eq. (18)) shrinks if the macroions get closer to the wall. This is due to the increasing counterion concentration at embodied in $\rho_w(z)$ which keeps the additional counterions closer to the macroions.

In the spirit of density-functional perturbation theory, we insert this result for $\Delta(\vec{r}) \equiv \Delta^{(0)}(\vec{r}, \vec{R}_1)$ into the density functional $\mathcal{F}([\rho(\vec{r})], \{\vec{R}_1\})$ and get the effective force $\vec{F}_1$ acting on the macroion approximately as

$$\vec{F}_1 = -\vec{\nabla}_{\vec{R}_1} \mathcal{F}([\rho_w(z) + \Delta^{(0)}(\vec{r}, \vec{r}_1)], \{\vec{R}_1\}) \tag{20}$$

In leading order this turns out to be

$$\vec{F}_1 = -\vec{\nabla}_{\vec{R}_1} V_{\text{ext}}(Z_1) \tag{21}$$

where the external macroion potential is given by

$$V_{\text{ext}}(Z_1) = |Ze|\phi(Z_1) \tag{22}$$

Here $\phi(Z_1)$ is the PB-result of Eq. (5).

This result implies that the macroion–wall interaction is as expected from our macroion-free consideration of the last chapter. The additional counterions from the macroions do not alter this result since they are spherically symmetric around the macroion and their contribution averages out. We remark that the potential $V_{\text{ext}}(Z_1)$ can directly be measured by internal reflection microscopy [34]. Within the parabolic approximation (Eq. (6)), the macroion behaves as a Brownian oscillator in z-direction with a Gaussian macroionic density profile which can also be tested by experiment [3].

At this stage, we also remark that the force $\vec{F}_1$ is a counterion-averaged force, not an instantaneous force. It is this force with which one has to perform the additional macroion average [31] to obtain total statistical averages.

2.3. Two macroions between charged plate

Consider now a pair of macroions ($N_m = 2$) with positions $\vec{R}_1 = (X_1, Y_1, Z_1)$ and $\vec{R}_2 = (X_2, Y_2, Z_2)$ In this case, $\mathcal{F}^{(4)}([\rho(\vec{r})], \{\vec{r}_1\})$ from Eq. (14) has to be replaced with

$$\mathcal{F}^{(4)}([\rho(\vec{r})], \{\vec{R}_1, \vec{R}_2\}) = \int_\Omega d^3 r \rho(\vec{r}) \sum_{i=1}^{2} V_{\text{mc}}(|\vec{r} - \vec{R}_i|) \tag{23}$$

and the total functional now depends parametrically on $\vec{R}_1$ and $\vec{R}_2$, $\mathcal{F} \equiv \mathcal{F}([\rho(\vec{r})], \vec{R}_i, i = 1, 2)$. We now follow the same strategy as explained in the last section and chose as a reference density

$$\bar{\rho}_w(z) = \rho_w(z) + \bar{\rho} \tag{24}$$

where $\bar{\rho} = |Z/q|N_m/\Omega$ is the mean counterion density coming from the macroions. Expanding the non-linear part $\mathcal{F}^{(1)}[\rho(\vec{r})]$ of the functional as in Eq. (16), we again adopt the 'adiabatic approach' for $k_B T(\Delta(\vec{r})/\bar{\rho}_w(z))$ (with $\Delta\vec{r} \equiv \rho(\vec{r}) - \bar{\rho}_w(z)$) and approximate $\bar{\rho}_w(z)$ here by an averaged constant

$$\bar{\rho}_w(z) = \bar{\rho} + \frac{1}{Z_2 - Z_1} \int_{Z_1}^{Z_2} \mathrm{d}z \rho_w(z) \equiv \tilde{\rho}(Z_1, Z_2) \tag{25}$$

Again, as in Eq. (18), the minimizing counterion density $\rho^{(0)}(\vec{r}, \{\vec{R}_i\}, i = 1, 2)$ consists then of Yukawa orbitals centered around the macroions with an inverse Debye–Hückel screening length given by

$$\kappa(Z_1, Z_2)^2 = \frac{4\pi(qe)^2 \tilde{\rho}(Z_1, Z_2)}{\epsilon k_B T} \tag{26}$$

i.e.

$$\rho^{(0)}(\vec{r}, \{\vec{R}_i\}, i = 1, 2) \approx \rho_w(z + \sum_{i=1}^{2} |\frac{Z}{q}| \kappa(Z_1, Z_2)$$

$$4\pi \frac{\exp(-\kappa(Z_1, Z_2)|\vec{r} - \vec{R}_i|)}{|\vec{r} - \vec{R}_i|} \tag{27}$$

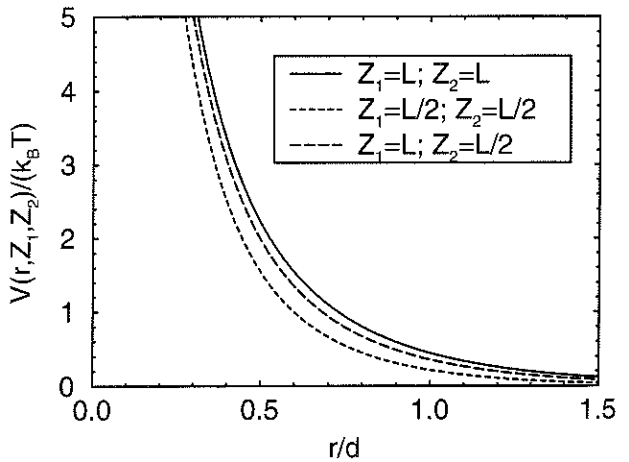

Fig. 4. Interaction potential $V(r,Z_1,Z_2)$ between two particles for run A vs. their separation r in units of an average separation d (d is the nearest-neighbour separation in a 2-dimensional triangular lattice of the same density). The solid curve corresponds to two particles in the mid-plane ($Z_1 = Z_2 = L$), the short-dashed curve to two particles at $Z_1 = Z_2 = L/2$, and the long-dashed curve to one particle in the mid-plane ($Z_1 = L$) and one at $Z_2 = L/2$.

Inserting this result into the density functional we obtain in leading order for the effective forces $\vec{F}_i$ acting onto the macroions

$$\vec{F}_i = \vec{\nabla}_{\vec{R}_i} \mathcal{F}([\rho(\vec{r})], \{\vec{R}_i\}, i=1,2)$$

$$= -\vec{\nabla}_{\vec{R}_i} \left[V_{\text{ext}}(Z_i) + \frac{Z^2 e^2}{\epsilon} \frac{\exp(-\kappa(Z_1,Z_2)|\vec{R}_1 - \vec{R}_{2_i}|)}{|\vec{R}_1 - \vec{R}_2|} \right] \quad (28)$$

Consequently, the macroions interact via a Yukawa pair potential with a space-dependent screening since κ depends explicitly on Z_1 and Z_2. On the other hand, the macroion–wall interaction stays the same as for a single macroion.

2.4. N_m macroions between charged orate

Finally we consider an arbitrary number of macroions. We assume that the interaction is pairwise and given by the space-dependent Yukawa pair potential as described by Eq. (28). The only difference as compared to the last section is that there is now a finite counterion concentration from the macroions since they possess a finite number density $\rho_m = N_m/\Omega$. Let us state the final model we shall investigate by computer simulation in the following section.

N_m macroions with a finite number density ρ_m interact with the plates via the external potential

$$V_{\text{ext}}(Z_1) = \begin{cases} \infty & \text{for } z < 0 \text{ and } z > 2L \\ 0 - |Ze| \dfrac{2k_B T}{|qe|} \ln(\cos(\gamma 0(1 - z/L))) & \text{for } 0 \le z \le 2L \end{cases} \quad (29)$$

Among themselves they interact via a space-dependent Yukawa Pair potential

$$V(\vec{R}_1, \vec{R}_2) = \frac{Z^2 e^2}{\epsilon} \frac{\exp(-\kappa(Z_1,Z_2)|\vec{R}_1 - \vec{R}_{2_i}|)}{|\vec{R}_1 - \vec{R}_2|} \quad (30)$$

$\vec{R}_1$ and $\vec{R}_2$ denoting the positions of the particle pair and

$$\kappa(Z_1,Z_2)^2 = \frac{4\pi(qe)^2 \tilde{\rho}(Z_1,Z_2)}{\epsilon k_B T} \quad (31)$$

where

$$\tilde{\rho}(Z_1,Z_2) = |Z/q|\rho_m + \frac{1}{Z_2 - Z_1} \int_{Z_1}^{Z_2} dz \rho_w(z) \quad (32)$$

This means that $\kappa(Z_1, Z_2)$ is the root mean square between the wall–counterion contribution and that stemming from the 'macroionic' counterions. In the limit of neutral plates ($\rho \equiv 0$), we recover again the usual space-independent screening κ given by the counterions coming from the macroions. In Fig. 4, the space-dependent pair potential as obtained from Eq. (30) is shown for different coordinates Z_1 and Z_2 of the macroion pair. As expected, the potential depends sensitively on these z-coordinates. We finally note that our model was not obtained by a systematic approximation but the physical screening mechanism is incorporated, at least qualitatively. As in the case of the bulk potential of DerJaguin-Landfau-Verwey-Overbeek (DLVO) [35,36], we expect, however, that the range of its applications is wider than expected from its theoretical derivation as long as one deals with renormalized parameters.

We finally crudely model and include in our calculations also the effect of a van der Waals attraction between the plates and the particles. If the particles are index-matched with the solvent, the van der Waals interaction between the particles is small. In a typical experimental set-up (glass plates and aqueous solutions), the polarizabilities of the walls and the particles is quite different. This gives rise to an additional external van der Waals potential. We simply include this attraction by adding a parabolic term $b(z - L)^2$ ($b < 0$) to the external potential (Eq. (29)). The most extreme case is that where $b \equiv b_c$ exactly cancels the quadratic term in the expansion of Eq. (6) which means that the total external potential starts with a contribution $\propto (z_L)^4$ for $z \approx L$. The total external potential $V_{\text{ext}}(Z)$ is shown in Fig. 5 for these two extreme cases ($b = 0$ and $b = b_c$).

3. Results of computer simulation

We performed standard molecular-dynamics simulations (see e.g. Ref. [37]) with $N_m = 500$ macroions in a periodically repeated quadratic box in lateral direction. The timestep was chosen such that the conservation of the total energy was granted. After every 100 timesteps, the velocities were scaled in order to reproduce the prescribed temperature. For the parameters we used room temperature ($T = 300$ K), and the dielectric constant was $\epsilon = 10$. The counterions are monovalent ($q = 1$) and the macroion charge number was $Z = 100$. The walls have a charge density $\sigma = 0.13e/\text{nm}^2$ and are separated by $2L = 0.005$ cm. For run A the density of macroions was such that the screening by 'macroionic' counterions was $2L\kappa_m = 1$, where $\kappa_m = 4\pi\rho_m Z q e^2/(\epsilon k_B T)$. For run B this screening was $2L\kappa_m = 0.2.1$

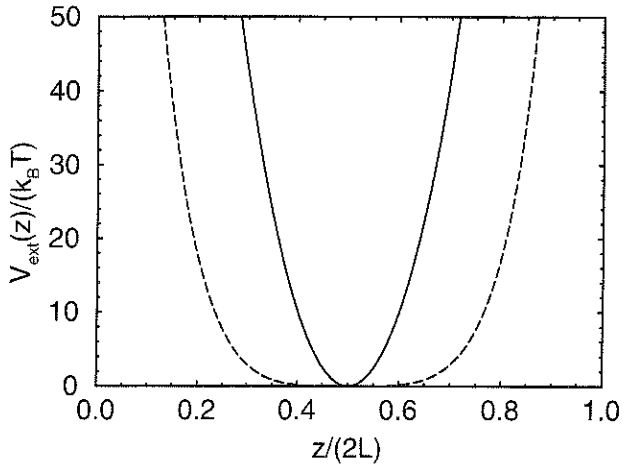

Fig. 5. Potential energy $V_{\text{ext}}(z)$ for particles of charge $Z = 100$ between charged walls as in Fig. 2. The solid curve corresponds to the electrostatic wall interaction alone, the dashed curve to an electrostatic wall interaction, the quadratic term of which is fully compensated by a wall attraction.

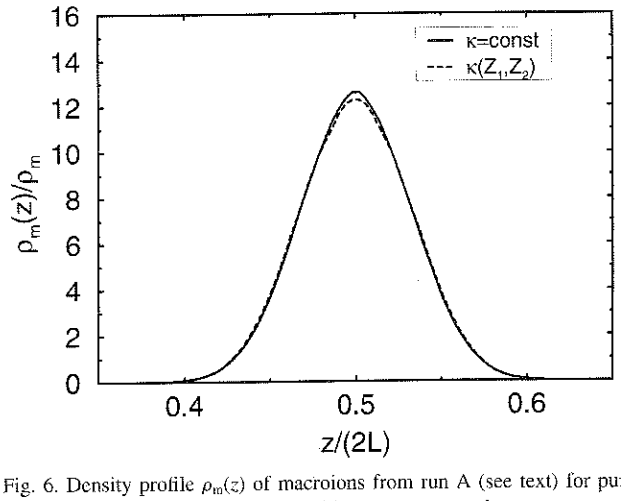

Fig. 6. Density profile $\rho_m(z)$ of macroions from run A (see text) for pure electrostatic wall interaction. The solid curve corresponds to a constant κ, the dashed curve to a space-dependent κ.

Our target quantity is the macroionic density profile $\rho_m(z)$ between the plates. In Fig. 6, we have plotted $\rho_m(z)$ in the case of absence of van-der-Waals attraction ($b = 0$) for a typical parameter combination. The counterion density for calculations with space-independent κ is taken to be the same as that for the space-dependent case at $z = L$.

Comparing our results for the space-dependent potential (dashed line) with that of the traditional space-independent potential (solid line), one realises that the results are very close. In fact, the repulsion from the charged walls is so large that the macroions practically stay within a monolayer. Consequently, effects of the space-dependent screening are much reduced. The same result was obtained for different other parameter combinations, proving that the traditional Yukawa picture with constant inverse screening length κ is justified. Nevertheless one can see small deviations: the midplane density is a little reduced and the wings are slightly more pronounced for the space-dependent screening.

The situation, however, can become different if the van der Waals attraction between the walls and the macroions is strong enough to pull the particles closer to the walls. Results for the extreme case $b = b_c$ where the quadratic term in $V_{ext}(z)$ vanishes are shown in Fig. 7 for two different parameter combinations. Here, indeed, for the same parameters as those in Fig. 6, there are stronger deviations in the wings and in the mid-plane density. This is only the case, however, if the structure is strongly influenced by inter-particle interactions. For low particle densities (run B) the profiles are determined mainly by the particle–wall interaction, and are therefore largely independent of the model.

4. Discussion and conclusions

In conclusion, we have investigated the inhomogeneous screening induced by the wall counterions in calculating the effective interaction between out-of-midplane macroions. I only electrostatic interactions are taken into account, the macroionic density profiles were practically indistinguishable from those of the space-independent pair potential This justifies the Yukawa-picture used in previous calculations. However, if a strong van der Waals attraction is present, the macroionic density profiles can be affected by the space-dependent screening. In particular, the mid-plane density is reduced and the wings are more extended towards the walls.

Effects of the space-dependent pair potential may further alter the freezing properties with respect to the usual space independent Yukawa potential, and may eventually explain the stability of near-wall crystallites which were recently found experimentally [17]. However, more theoretical work is still needed in this direction.

It is clear that we have ignored several effects in our theoretical derivation including the finite macroion core effect of added salt ions, and the effect of image charge [18–20,38] which are important if the dielectric constants of the plates and the solvent are different. A finite macroionic core would result in an effective macroion charge depending on the core size as known from the bulk macroionic case [35]. However, we leave a detailed calculation justifying this for future studies. Our linear screening theory furthermore only applies for diluted suspensions. To overcome this restriction, one has to do more sophisticated calculations. It would be interesting to apply the ab initio computer simulation technique of Ref. [31] to confined colloids or to do Monte-Carlo simulations of the primitive mode with only few macroions along the lines of Ref. [39], in order to test our interaction mode and to incorporate non-linear counterion screening effects arising from a high macroion concentration.

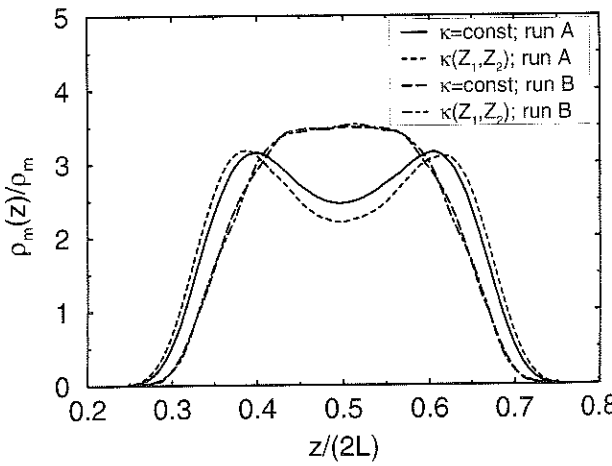

Fig. 7. Density distribution of macroions for an electrostatic wall interaction, the quadratic term of which is fully compensated by a wall attraction. The solid curve corresponds to run A (see text) and a constant κ, the short-dashed curve to run A and a space-dependent κ, the long-dashed curve to run B and a constant κ, and the dot-dashed curve to run E and a space-dependent κ.

Acknowledgements

We thank J. Chakrabarti, A.R. Denton and B. Weyerich for helpful remarks.

References

[1] D.G. Grier, C.A. Murray, in A.K. Arora, B.V.R. Tata (eds.), Ordering and Phase Transitions in Charged Colloids, VCH, New York, 1996, p. 69.
[2] W. Schaertl, H. Sillescu, J. Colloid Interface Sci. 155 (1993) 313.
[3] G.M. Kepler, S. Fraden, Langmuir 10 (1994) 2501.
[4] K.J. Strandburp, Rev. Mod. Phys. 60 (1988) 161.
[5] C.A. Murray, D.H. van Winkle, Phys. Rev. Lett. 58 (1987) 1200.
[6] C.A. Murray, R.A. Wenk, Phys. Rev. Lett. 62 (1989) 1643.
[7] C.A. Murray, W.O. Sprenger, R.A. Wenk, Phys. Rev. B 42 (1990) 688.
[8] D.G. Grier, C.A. Murray, J. Chem. Phys. 100 (1994) 9088.
[9] A.H. Marcus, S.A. Rice, Phys. Rev. Lett. 77 (1996) 2577.
[10] A.H. Marcus, S.A. Rice, Phys. Rev. E 55 (1997) 63.
[11] R.E. Kusner, J.A. Mann, J. Kerins, A.J. Dahms, Phys. Rev. Lett. 73 (1994) 3113.
[12] R.E. Kusner, J.A. Mann, A.J. Dahms, Phys. Rev. B 51 (1995) 5746.
[13] G.M. Kepler, S. Fraden, Phys. Rev. Lett. 73 (1994) 356.
[14] J.C. Crocker, D.G. Grier, Phys. Rev. Lett. 73 (1994) 352.
[15] A.E. Larsen, D.G. Grier, Phys. Rev. Lett. 76 (1996) 3862.
[16] J.C. Crocker, D.G. Grier, Phys. Rev. Lett. 77 (1996) 1897.
[17] A.E. Larsen, D.G. Grier, Nature 385 (1997) 230.
[18] E. Chang, D.W. Hone, Europhys. Lett. 5 (1988) 635.
[19] E. Chang, D.W. Hone, Phys. Rev. A 38 (1988) 582.
[20] E. Chang, D.W. Hone, J. Physique France 49 (1988) 25.
[21] M. Medina-Noyola, B.I. Ivlev, Phys. Rev. E 52 (1995) 6281.
[22] H. Löwen, J. Phys. Condens. Matter 4 (1992) 10105.
[23] H. Löwen, J. Phys. Condens. Matter 5 (1993) 2649.
[24] M. Chávez-Páez, J.M. Méndez-Alcaraz, J.L. Aranz-Lara, M. Medina-Noyola, J. Colloid Interface Sci. 179 (1996) 426.
[25] M.D. Carbajal-Tinoco, F. Castro-Román, J.L. Arauz-Lara, Phys. Rev. E 53 (1996) 374.
[26] B. Löhle, R. Klein, Physica A 235 (1997) 224.
[27] B. Cichocki, B.U. Felderhof, J. Phys. Condens. Matter 6 (1994) 7287.
[28] H. Aranda-Espinoza, M. Carbajal-Tinoco, E. Urrutia-Banuelos, J.L. Arauz-Lara, M. Medina-Noyola, J. Chem. Phys. 101 (1994) 10925.
[29] H. Löwen, Phys. Rev. E 53 (1996) R29.
[30] K.J. Naidoo, J. Schnitker, J. Chem. Phys. 100 (1994) 3114.
[31] H. Löwen, J.P. Hansen, P.A. Madden, J. Chem. Phys. 98 (1993) 3275.
[32] W.B. Russel, D.A. Saville, W.R. Schowalter, Colloidal Dispersions, Cambridge University Press, Cambridge, 1989.
[33] K.S. Schmitz, Macroions in Solution and Colloidal Suspension, VCH, New York, 1993.
[34] D.C. Prieve, N.A. Frej, Langmuir 6 (1990) 396.
[35] B.V. Derjaguin, L.D. Landau, Acta Physicochim. USSR 14 (1941) 633.
[36] E.J.W. Verwey, J.T.G. Overbeek, Theory of the Stability of Lyophobic Colloids, Elsevier, Amsterdam, 1948.
[37] M.P. Allen, D.J. Tildesley, Computer Simulation of Liquids, Clarendon Press, Oxford, 1989.
[38] A. Krämer, M. Vossen, F. Forstmann, J. Chem. Phys. 106 (1997) 2792.
[39] I. D'Amico, H. Löwen, Physica A 237 (1997) 25.